Accepted Manuscript

Investigations of mechanical, thermal and morphological properties of FDM fabricated parts for friction welding applications

Ranvijay Kumar, Rupinder Singh, IPS Ahuja

PII: S0263-2241(18)30092-7
DOI: https://doi.org/10.1016/j.measurement.2018.02.006
Reference: MEASUR 5254

To appear in: *Measurement*

Received Date: 27 October 2017
Revised Date: 27 January 2018
Accepted Date: 6 February 2018

Please cite this article as: R. Kumar, R. Singh, I. Ahuja, Investigations of mechanical, thermal and morphological properties of FDM fabricated parts for friction welding applications, *Measurement* (2018), doi: https://doi.org/10.1016/j.measurement.2018.02.006

Investigations of mechanical, thermal and morphological properties of FDM fabricated parts for friction welding applications

[1,2]Ranvijay Kumar [1]Rupinder Singh*, [2]IPS Ahuja

[1]Dept. of Production Engineering, Guru Nanak Dev Engineering College, Ludhiana (India)

[2]Dept. of Mech. Engineering, Punjabi University, Patiala (India)

[1,2]ranvijayk12@gmail.com [1]rupindersingh78@yahoo.com ,[2]ahujaips@gmail.com

*Corresponding author

Abstract

Friction welding is one of the solid state welding techniques, for which the two pieces of thermoplastic materials must be compatible to each other. Friction welding of the two similar thermoplastic is an easy exercise but joining two dissimilar thermoplastic is difficult because of large differences in viscosity, specific density, molecular weight, melting point, crystalline vs. amorphous nature, surface behavior and dynamic-mechanical properties. In last three decades, studies have been reported to perform the friction and friction stir welding of thermoplastics but still the reason for compatibility of thermoplastic is not understood properly. In the present study attempts have been made to perform the compatibility analysis of two dissimilar polymers namely; acrylonitrile butadiene styrene (ABS) and polyamide 6 (PA6) by establishing their melt flow properties after Aluminum (Al) metal powder reinforcement. Twin screw extrusion (TSE) and fused deposition modeling (FDM) technologies were used to fabricate the welding specimen for potential application in maintenance engineering.

Keywords: Mechanical, Thermal, Morphological, Fused Deposition Modelling, Twin screw extrusion

1. Introduction

Thermoplastics are characterized by their nature of exhibiting physical, chemical, mechanical, thermal and morphological properties such as; fracture resistive capacity, amorphous vs. crystalline, melting and glass transition temperature, surface behavior, carbon chain length, molecular arrangement, and molecular weight vs. molecular density. Dissimilar thermoplastic material posses non-compatibility issues which hinders to apply it in different application; especially where application of thermoplastic needs to be the compatible by characteristics (e.g.

solid state welding) [1-5]. So considering toward fixation of these issues some of the studies revealed the mechanism, theory and techniques by which two dissimilar thermoplastic material can be characterized, e.g. reinforcement of metallic and non-metallic fillers leads to the improvement in the mechanical and morphological characteristics of the polymer matrix as well as polymer compatibility for joining and mixing [6-8]. The dissimilar polymeric based materials often face a problem like mixing to each other or say their compatibility. Some researchers have studied the effect of metallic, non-metallic compounds at micron or nano-size level to enhance the compatibility, mixing and thermal stability [9-11]. Besides mechanical mixing of polymers matrix with fillers, the chemical mixing in controlled chemical proportion offers the better blend of polymer matrix for thermal, mechanical and metallographic properties. The chemical mixing reduces the porosity, improves the packing factors [12-13]. For the specific cases of the friction welding applications, the FDM can be used for the fabrication of the consumable tool which will use for joining of polymeric sheets. For example, pipelines are generally made up of the thermoplastic material and occurrence of cracks and leakages are the most common things which cause material loss, time loss and economic loss. To prevent these problems a rapid tool as drill bit can be applied to fix these issues. The researcher in present era aims for welding of dissimilar polymers. Some studies have reported the mechanism of friction welding for dissimilar polymeric material like; ABS and high density polyethylene (HDPE), low density polyethylene (LDPE), Polypropylene (PP), Polycarbonate (PC), Polyamide (PA) and etc [14]. Some of the studies have outlined the advancement in the process to check the feasibility of the different solid state welding concept for thermoplastic material. The reinforcement in the form of metals, nonmetals and composite alloys can enhance the weldability [15-19]. Recent studies have highlighted the use of different tools and technique to explain the effect of tool pin profile, a heating assisted tool and effects of particulate on tensile properties [20-22].

As per reported literature, researchers have performed lot of work in field of friction welding, extrusion process, part fabrication by FDM. Also number of studies has been reported for friction welding of thermoplastic which hold the technical evaluation from the mechanical, thermal and morphological properties view point. But hitherto no study has been reported that can explain compatibility of two dissimilar thermoplastic materials and how to make polymeric material compatible to each other especially for solid state welding applications. In the present study attempts have been made firstly to enhance compatibility by establishing their melt flow properties (in a particular range), and then supported by screw extrusion and FDM it was tried to fabricate the parts for rapid monitoring and repair applications through friction welding.

2. Experimentations

Firstly two cylindrical pieces ABS and PA6 of dimension 30mm diameter and 50mm length was fabricated on the FDM setup. Fabricated part was then put on the lathe machine and exposed to frictionally attach at rotational speed of 1200rpm, 0.045mm/rev of federate and 10sec of stirring time. The welding/joining of the parts were failed and parts were not joined to each other (may be due to their differences in the rheological and thermal properties). So next it was tried to enhance the compatibility of mentioned thermoplastic by varying Al content reinforcement by maintaining their melt flow properties.

2.1 Materials and methods

ABS and PA6 thermoplastic have been selected for the experimentation purposes because of their significant differences in mechanical, thermal, chemical and morphological properties. ABS is characterized as amorphous whereas PA6 is semi-crystalline natured, ABS is having low chemical resistivity whereas PA6 having excellent chemical resistivity, melting point of PA6 is as high as compared to the ABS. mechanical strength of the PA6 is higher as compared to the ABS. so, considering said differences it is required to have enhanced the compatibility of these thermoplastic in terms of rheological and thermal properties. ABS and PA6 thermoplastic was purchased from Batra polymer Pvt. Ltd, Ludhiana, India having granules size of 2mm. The Al powder was selected to characterize the melt flow property of having measured the grain size of 50mmicrons purchased from Shivas chemicals Pvt. Ltd. Ludhiana, India. The mechanical properties of the ABS and PA6 were investigated after preparation of 1.5mm diameter feedstock filament from the TSE keeping temperature of 230^{o}C and 30rpm screw speed. The mechanical properties have been obtained as shown in Table 1.

Table 1 Mechanical properties investigated for ABS and PA6 (Extruded)

Polymer	PL (N)	BL (N)	PS(Kg/mm^2)	BS Kg/mm^2)	PE (mm)	BE (%)	%PE	%BL	E (MPa)	σ (MPa)
ABS	8.6	7.74	3.791	3.412	2.85	3.04	4.38	4.38	55.29	2.28

PA6	14.1	12.69	7.016	6.315	6.84	7.41	10.52	11.40	35.39	0.13

PL- Peak load, BL- Break load, PS- Peak strength, BS- Break strength, PE- Peak elongation, BE- Break elongation, E- Young's modulus, σ- Yield stress.

DSC tests were performed under 30-250°C temperature range with 10°C/min heating rate under the N_2 gas supply of 50ml/min. DSC curves are plotted as shown in Fig. 1 under 2 cycle of heating. The DSC was performed under the two cycles because after the first heating cycle material becomes stable in nature and results in the correct material information in 2nd cycle of heating and cooling. So as is second cycle of heating the melting point of ABS was measured as 201.22°C and during cooling phase, solidification temperature of 111.78°C was calculated.

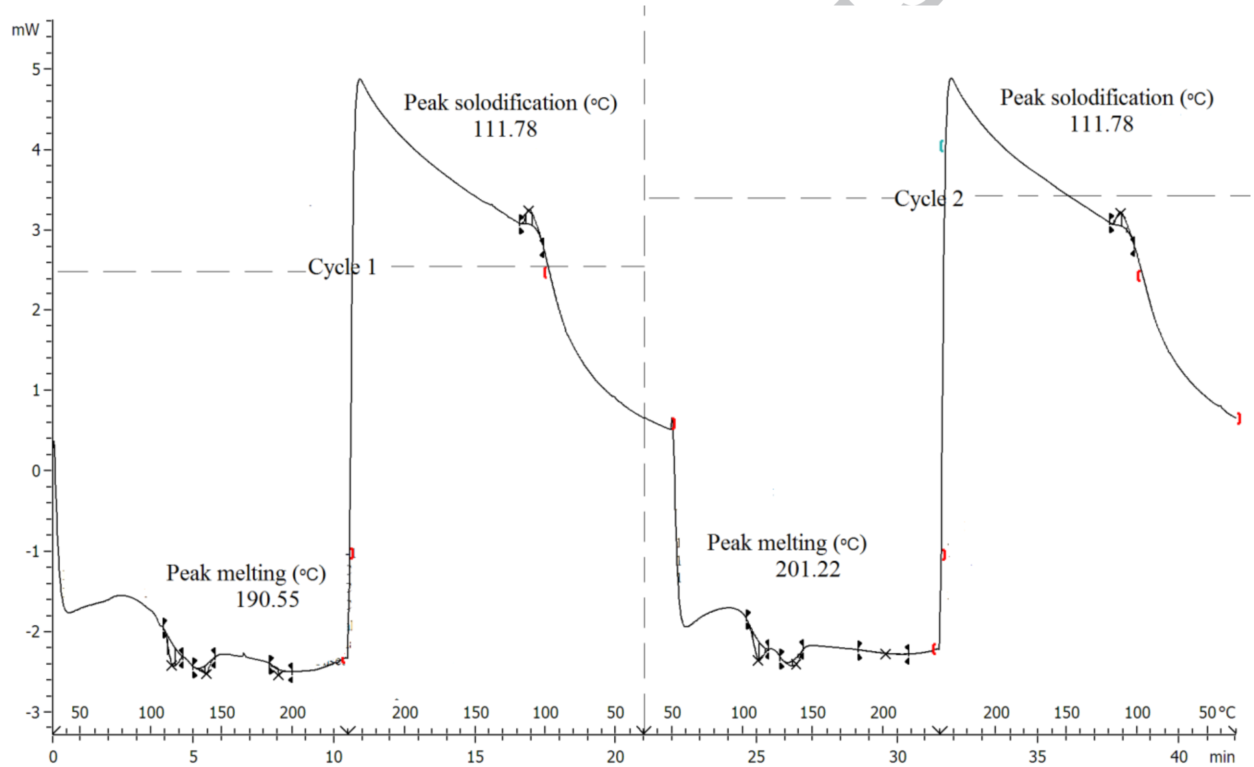

Fig. 1 DSC of ABS granules

Similarly taking all the DSC input same, melting behavior of PA6 was evaluated. The results of 1st cycle were neglected because polymer takes 1st heating cycle to become thermally stabilize. So interpretations of 2nd heating and cooling cycle are considered as most stable. PA6 was having the peak melting point of 219.35°C whereas peak solidification point of 189.03°C (See Fig. 2 of 2nd cycle).

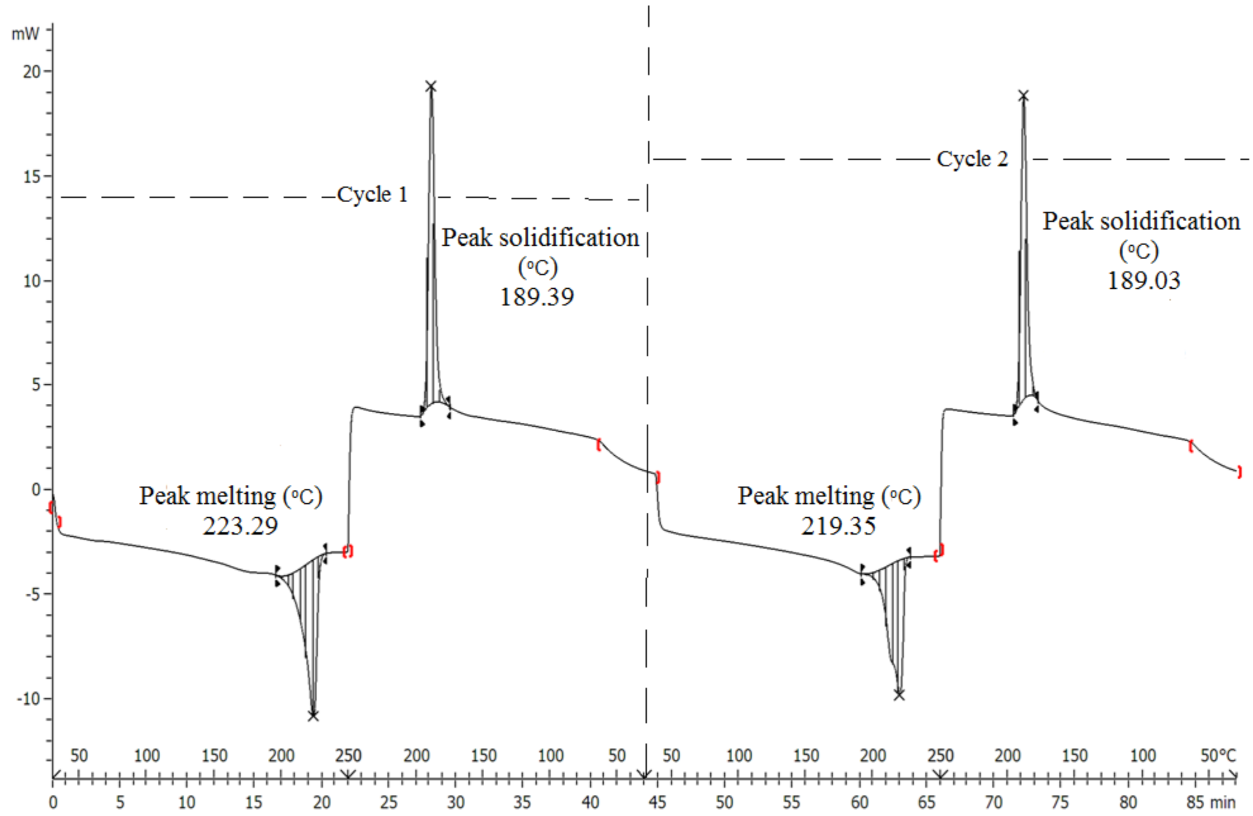

Fig. 2 DSC of ABS granules

2.2 Melt flow index (MFI)

MFI is one of the rheological properties and indexes to determine the flow characteristics of the thermoplastic material under certain heating and loading conditions [23]. A number of studies have been reported to determine the connection among MFI, mechanical and thermal and chemical properties [24-29]. In the present study ASTM D1238 standard was used to evaluate the MFI of ABS and PA6 with different reinforcement level of Al powder. A standard weight of 3.8Kg and temperature of 230^{o}C was fixed to calculate the MFI in g/10min.

Al content were varied from 5% up to 50% resulted in significant changes in the MFI of ABS and PA6 polymer matrix. It was observed that a similar range of MFI obtained by ABS with 15% Al content (11.57 g/10min) andPA6 with 50% Al content (11.97 g/10min). So based upon the pre-determined hypotheses it was considered that ABS-15Al and PA-50Al are compatible based upon melt flow property as one of the rheological properties (See Fig. 3).

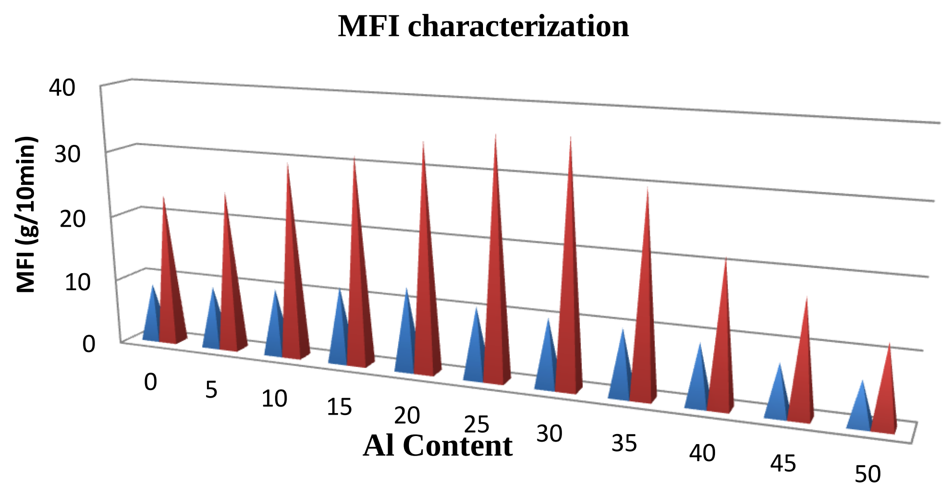

	0	5	10	15	20	25	30	35	40	45	50
MFI with ABS	8.76	9.4	10.12	11.57	12.64	10.82	10.28	9.99	9.14	7.56	6.48
MFI with Nylon6	23.27	24.52	29.82	31.62	34.4	36.01	36.37	30.07	21.52	17.07	11.97

Fig. 3 MFI evaluation with varying Al content

2.3 Twin screw extrusion

Towards fabricating feedstock filaments of ABS-15Al and PA6-50Al composition there is a requirement of producing feedstock filaments for FDM machine. So feedstock filaments of said composition were prepared on TSE (Co-axial co-rotating type manufactured by Thermo Fisher Scientific). The TSE setup was having the extrude nozzle diameter of 1.5mm, operating temperature range of 30-400^{o}C, rotational speed of 0-400rpm (see Fig. 4).

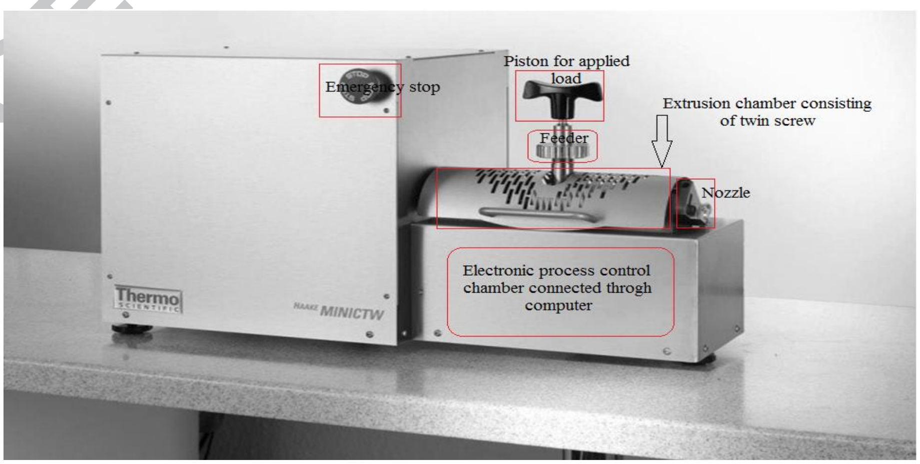

Fig, 4 Configurations of TSE setup

Based upon the trial experimentation it was observed that under certain parametric conditions feedstock filaments resulted in uniform longitudinal dimension. So based upon uniformity feedstock filament for FDM have been prepared under parametric combinations given in Table 2.

Table 2 Input process parameters for extrusion of thermoplastics

Parameter	ABS-15Al	PA6-50Al
Temperature(^{o}C)	220	245
Applied Load(Kg)	20	20
Screw Speed(RPM)	30	15

2.4 Fused Deposition modeling

After preparation of feedstock filaments of ABS-15Al and PA6-50Al, parts was prepared for friction welding application considering some static parametric and some variable parametric conditions. Static parameter conditions are shown in Table 3.

Table 3 Static input parameters for part fabrication through FDM

Process variable	Operating condition
Nozzle diameter	0.3mm
Filament diameter	1.75mm
Layer height	0.4mm
Solid layers	Top-3, Bottom-3
Fill pattern	Honeycomb
Perimeter speed	30mm/sec
Infill speed	60mm/sec
Travel speed	130mm/sec
Extruder temperature	250^{o}C
Bed Temperature	55^{o}C

After fixing static parameter, variable parameters were selected (based upon pilot study) as infill density, no. of perimeters and nozzle angle because these can be the major variable toward change in the strength and surface characteristic of the final products. Table 4 shows variable parameters and their levels.

Table 4 Variable input process parameters

Parameters	level
Infill Density (%)	0.6, 0.8, 1.0
Perimeters (number)	4, 5, 6
Nozzle angle (^{0})	45, 60, 75

Note: Infill density: 0.6 means 60%, 0.8 means 80% and 1.0 means 100%

3.5 Design of experiments

Considering 3 different variable parameters and their levels as shown in Table 4, a Taguchi design of L9 orthogonal arrays have been developed to fabricate parts of ABS-15Al and PA6-50Al. Table 5 shows the developed Taguchi L9 orthogonal arrays.

Table 5 Taguchi L9 orthogonal arrays for fabrication of ABS-15Al and PA6-50Al parts.

Experiment no.	**Infill density** (%)	**Perimeters** (number)	**Nozzle angle** (^{0})
1	0.6	4	45
2	0.6	5	60
3	0.6	6	75
4	0.8	4	60
5	0.8	5	75
6	0.8	6	45
7	1.0	4	75
8	1.0	5	45
9	1.0	6	60

Configuring the different set of experiment according to Taguchi L9 orthogonal arrays, a .STL file was generated with designing software with following dimension description given in Fig. 5 and Table 6. The parts were fabricated of tensile specimen following the ASTM D638 type IV standard (See Fig. 5)

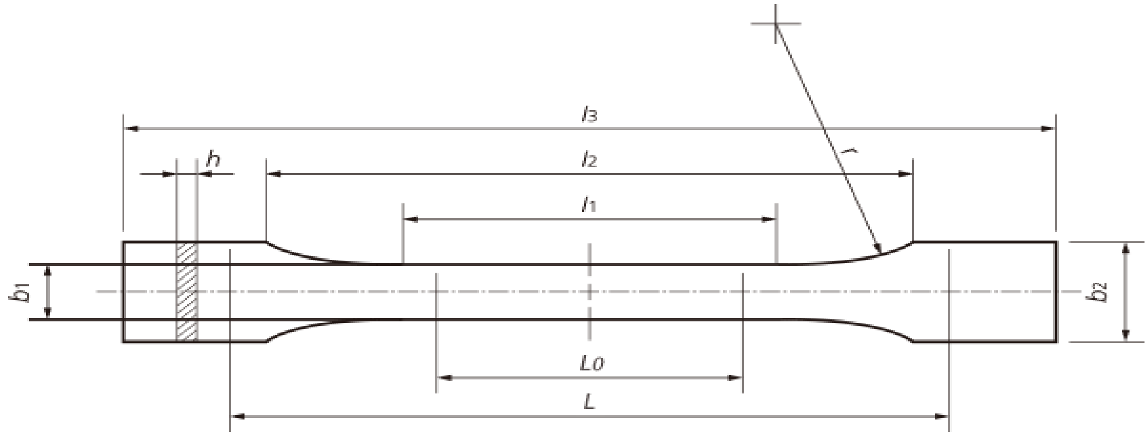

Fig. 5 Dimensional descriptions of ASTM D638 type IV tensile specimen

Fig. 6 shows the software designed 3D part of tensile specimen and FDM setup for fabrication.

Table 6 Dimensional description according to ASTM D 638 type IV tensile specimen

Size	Type IV (mm)
Full length, l_3	115
Parallel length, l_2	33
Gauge length, l_1	25
Parallel section width, strong$_1$	6
Thickness, h	4
Grip section width, strong$_2$	19
Distance between grip	65

Fig. 6 Designed specimen and FDM setup for part fabrication

Following design of experiment of Table 5, there are 9 tensile specimens (each for ABS-15Al and PA6-50Al) have been fabricated and employed for further testing of dimension, mechanical strength and morphology (See Fig. 7)

ABS-15Al PA6-50Al

Fig. 7 FDM fabricated parts of ABS-15Al and PA6-50Al

3. Results and discussions

Mechanical (peak load, peak strength, and yield stress) , thermal (melting point) and Scanning electron microscopy (SEM) observations have been performed to check the compatibility between selected composition of ABS-15Al and PA6-50Al.

3.1 Thermal analysis

Thermal analysis was performed by DSC resulted in an extraordinary observation regarding material compatibility. Comparative DSC of 4 samples has been taken for ABS, ABS-15Al, PA6 and PA6-50Al with prospective of calculating melting points. As performed earlier DSC was performed under 2 cycles of heating and cooling. The 1st cycle was not considered as a final results because it is assumed that in 1st cycle foreign materials are need to be vanished and their bonding with polymer material is evaporated due to heating. So results in 2nd cycle were considered as thermally stable. It was initially observed that melting points of ABS and PA6 matrix was obtained 201.22^{o}C and 219.35^{o}C respectively. But after reinforcement of Al powder to 15% in ABS and 50% in PA6 leads to the melting point of 218.11^{o}C and 219.35^{o}C respectively (See Fig. 8). So it was observed that ABS-15Al and ABS-50Al have been attained a very similar range of melting point due to Al powder reinforcement and considered as the compatible polymer matrix thermally.

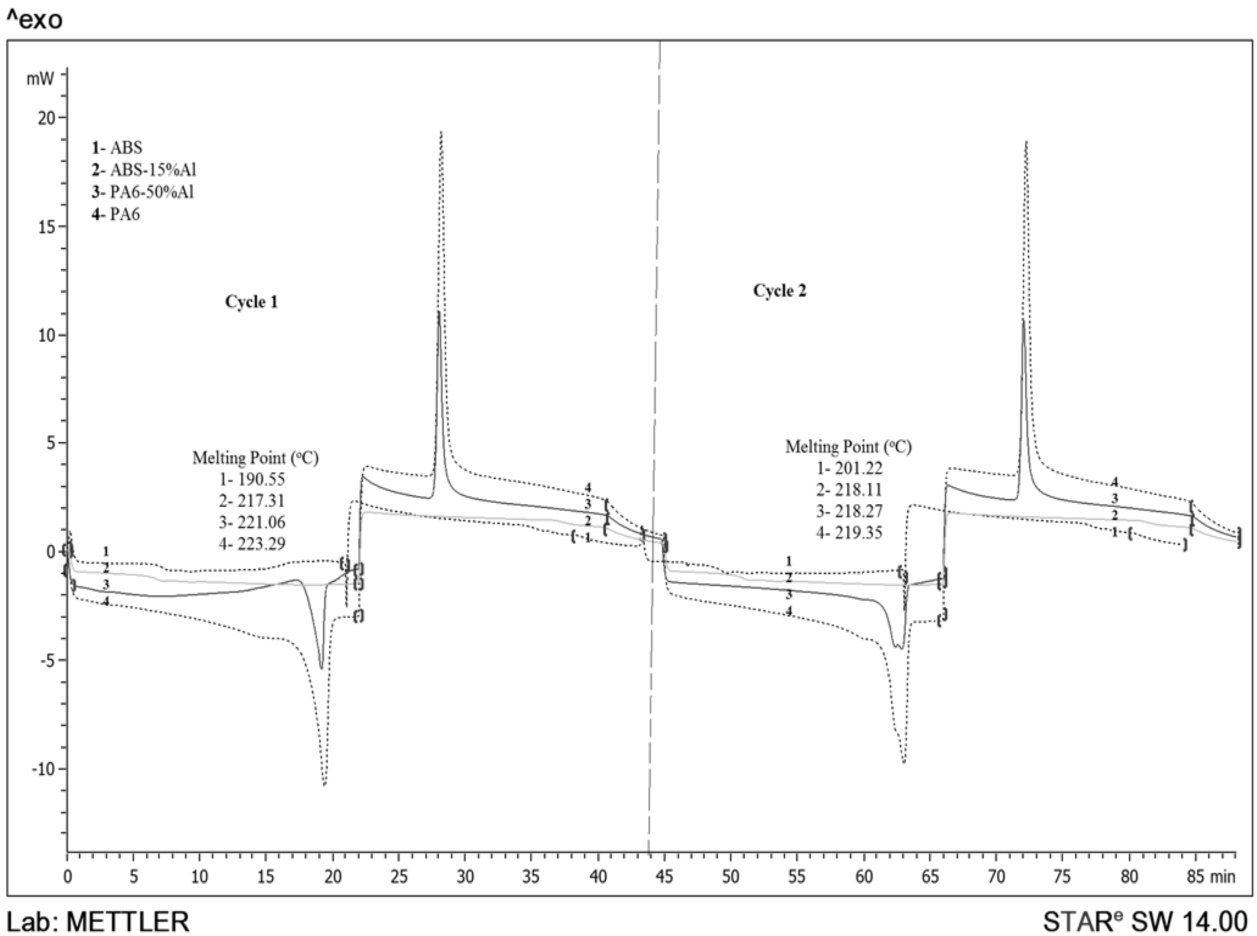

Fig. 8 Comparative DSC result for (1) ABS, (2) ABS-15Al, (3) PA6-50Al and (4) PA6

3.2 Tensile properties analysis

Following deign of experiment from Table 5 there are 9 parts are fabricated on FDM and further employed to universal tensile tester (ASTM D 1238). The tensile results were obtained after fracture of the specimen on tensile tester. Peak load, peak elongation and yield stresses as tensile properties have been selected as output process parameters for selection of best set of parameter of FDM. As observed from Table 7 (ABS-15AL) peak load (577.2N) was resulted maximum value at experiment no. 6, peak strength (22.43kgf/mm^2) at experiment no. 3 as desired whereas yield stress was obtained minimum (0.08MPa) at experiment no. 3.

Table 7 Mechanical properties of FDM printed ABS-15Al parts

Exp. no.	peak load (N)	SN ratio(dB)	peak Strength (kgf/mm^2)	SN ratio(dB)	yield stress (MPa)	SN ratio(dB)
1	419.4	52.4526	16.26	24.2224	0.04	1.5062
2	501.3	54.0020	18.47	25.3293	0.30	10.4576
3	538.4	54.6221	22.43	27.0166	0.08	21.9382
4	413.8	52.3358	15.41	23.7561	0.03	1.4806
5	508.9	54.1326	17.2	24.7106	0.15	16.4782
6	577.2	55.2265	20.72	26.3278	0.49	6.1961
7	427.1	52.6106	16.04	24.1041	0.39	8.1787
8	511.5	54.1769	19.06	25.6025	0.43	7.3306
9	561.1	54.9808	21.67	26.7172	0.30	10.4576

For PA-50Al parts prepared on FDM, Peak load (528.5N) and peak strength (22.02kgf/mm^2) was achieved maximum at experiment no. 4 whereas yield stress (0.14MPa) was achieved minimum at experiment no. 2 as desired (See Table 8).

Table 8 Mechanical properties of FDM printed PA6-50Al parts

Exp. no.	peak load (N)	SN ratio(dB)	peak Strength (kgf/mm^2	SN ratio(dB)	yield stress (MPa)	SN ratio(dB)
1	433.9	52.7478	18.08	25.1440	0.18	14.8945
2	512.4	54.1922	21.35	26.5880	0.14	17.0774
3	484.9	53.7130	20.2	26.1070	0.22	13.1515
4	528.5	54.4609	22.02	26.8563	0.4	7.9588
5	431.5	52.6996	19.98	26.0119	0.42	7.5350
6	465.8	53.3640	19.41	25.7605	0.4	7.9588
7	388.3	51.7833	16.18	24.1796	0.42	7.5350
8	322.6	50.1733	16.44	24.3180	0.48	6.3752
9	446.2	52.9906	18.59	25.3856	0.51	5.8486

3.2.1 Optimization of input process parameters

Every application of thermoplastics needs specific mechanical/tensile strength to fulfill the need. For examples for friction welding application it is desired to have the material with high load resistive capacities and low induced stresses. For such cases of variation specific properties optimized using present statistical mathematical model. It was observed that contributing towards SN ratios for best setting of maximizing the peak load fill density of 1.0, no. of perimeter 6 and nozzle angle of 45^{o} (See Fig. 9)

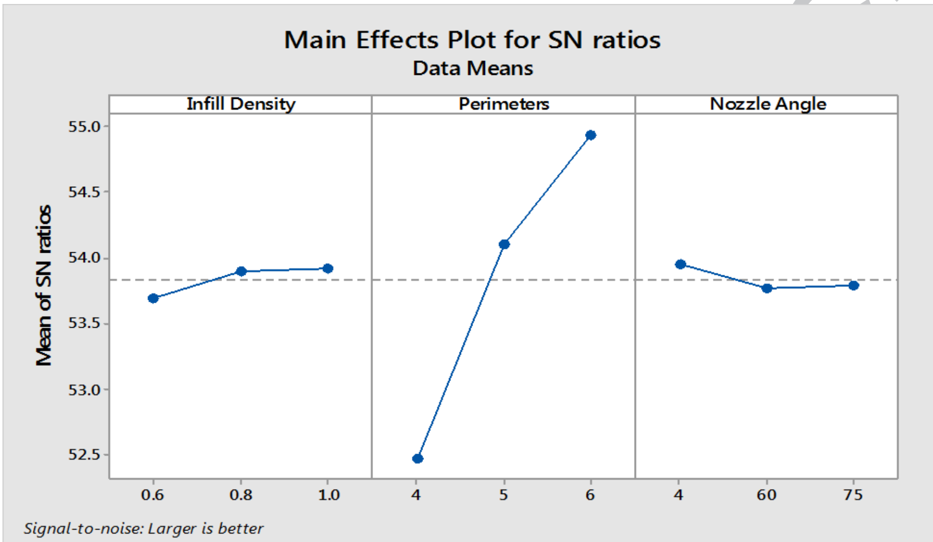

Fig. 9 Main effect plot for SN ratios of peak load (ABS-15Al)

Analysis of variance table (Table 9) suggested that no. of perimeter was the most contributing factor for change in peak load. It was observed that change of perimeter contributed 97.65% for the peak load whereas other two factors like infill density contributed 0.90% and nozzle angle contributed 0.60%. Probability (P) and Fisher coefficient (113.27) values was obtained 0.009 for perimeter suggested that perimeter was the most significant factor among all.

Table 9 Analysis of Variance for SN ratios

Source	DF	Seq SS	Adj SS	Adj MS	F	P	%age contribution
Infill Density	2	0.09624	0.09624	0.04812	1.15	0.466	0.90
Perimeters	2	9.52053	9.5205	4.76027	113.27	0.009	97.65
Nozzle Angle	2	0.05909	0.05909	0.02954	0.70	0.587	0.60

Residual Error	2	0.08405	0.08405	0.04203	0.85
Total	8	9.75991			

The Response Table (Table 10) was linked all the input parameters and calculate the delta values. The delta values were used to rank the order of parameter to be desired. The delta value was calculated by subtracting the lowest value form largest value. Perimeter was ranked 1, infill density was ranked 2 and nozzle angle was ranked 3.

Table 10 Response Table for Signal to Noise Ratios (Larger is better) for ABS-15Al

Level	Infill Density	Perimeters	Nozzle Angle
1	53.69	52.47	53.95
2	53.90	54.10	53.77
3	53.92	54.94	53.79
Delta	0.23	2.48	0.18
Rank	2	1	3

The optimum value of peak load in this case can be predicted by using following equation:

$\eta_{opt} = m+(m_{A3}–m) +(m_{B3}–m) +(m_{C1}–m)$ ....(i)

Where 'm' is the overall mean of SN ratio, m_{A3} is the mean of SN ratio for infill density at level 3, m_{B3} is the mean of SN ratio for perimeter at level 3,and m_{C1} is the mean of SN data for nozzle angle at level 1.

$y_{opt}^2 = (1/10)^{\eta opt/10}$ for properties, lesser is better

$y_{opt}^2 = (10)^{\eta opt / 10}$ for properties, greater is better

Considering peak load as maximum is better,

$y_{opt}^2 = (1/10)^{\eta opt/10}$ ……………….(ii)

Calculation:

Overall mean of SN ratios (m) for peak load was calculated as;

m = 53.83dB (See Table 7) ……………. (iii)

Now from response table of signal to noise ratio, mA3 = 53.92, m_{B3}=54.94, m_{C1}=53.95, (From Table 10)

Now from equation (i) and equation (ii)

η_{opt}= 53.83+(53.92-53.83) +(54.94-53.83) +(53.95-53.83)

η_{opt}= 55.15 ……………………….(iv)

Now, from equation (iv) $y_{opt}^2 = (10)^{\eta opt / 10}$

$y_{opt}^2 = (10)^{55.15/ 10}$

y_{opt} = 572.13N

The predicted optimum value for peak load (ABS-15%Al) = 572.13 N

So it was predicted that optimized peak load of 572.13 N will be obtained by keeping fill density 1.0, no. of perimeter 6 and nozzle angle of 45^o. The confirmatory experimentation was conducted on suggested setup and it was resulted in peak load of 571.87N very closer to the predicted values. Similarly all the tensile properties (Peak load, Peak strength and yield stress) was predicted and confirmed by experimentation optimally (for ABS-15Al and PA6-50Al) (See Table 11)

Table 11 Calculated/Predicted mechanical properties and experimentally determined values

Composition /Proportion	Attribute	Output parameters		
		Peak Load (N)	Peak strength (kgf/mm^2)	Yield stress (MPa)
ABS-15%Al	η_{opt}(dB)	55.15	26.99	24.38
	Predicted value(y_{opt})	572.13	22.36	0.06
	Best settings for predicted value	Density-1, perimeter-6, nozzle angle-45^o	Density-0.6, perimeter-6, nozzle angle-45^o	Density-1, perimeter-6, nozzle angle-75^o
	Actual value at optimized setup	571.87	22.55	0.06
PA6-50%Al	η_{opt}(dB)	54.99	27.06	16.045
	Predicted value(y_{opt})	561.69	22.54	0.25
	Best settings for predicted value	Density-0.6, perimeter-6, nozzle angle-60^o	Density-0.8, perimeter-6, nozzle angle-60^o	Density-0.6, perimeter-5, nozzle angle-60^o

	Actual value at optimized setup	560.12	25.03	0.24

3.2.2 Combined optimization of FDM process parameters

After optimizing specific output parameter for selection of optimized set of input parameters, it was optimized all the parameters in combined. The SN ratios for ABS-15Al and ABS-50Al were combined and main effect plot for SN ratios was plotted. It was observed after combining all the output parameters in ABS-15Al, giving maximum SN ration of 28.9929dB at experiment no. 6 whereas for PA6-50Al maximum values of SN ratio observed 2036 at experiment no. 6 (See Table 12)

Table 12 Combined SN ratios for FDM printed parts of ABS-15%Al and PA6-50%Al

Experiment no	Combined SN ratios (ABS-15%Al)	Combined SN ratios (PA6-50%Al)
1	25.4967	28.66
2	24.3393	29.18
3	28.9929	29.68
4	24.8927	29.51
5	27.2417	29.92
6	20.3280	30.36
7	22.4585	28.55
8	21.6589	29.34
9	24.4066	29.51

Main effect plot for SN ratios have been plotted against effect of input process parameters (Fill density, perimeter and nozzle angle) shown in Fig. 10. After combining SN ratio of all the parameters for ABS-15Al and PA6-50Al the most contributing set of input parameters have been selected for production of final parts. For parts of ABS-15Al, it was noted that 1.0 fill density, 6 perimeter and 75^{o} nozzle angle mostly contributed for SN ratio therefore this combination have been selected for fabrication of final product. Similarly for PA6-50Al, 1.0 fill density, 4 perimeter and 60^{o} nozzle was selected set of input parameter contributing towards better SN ratio.

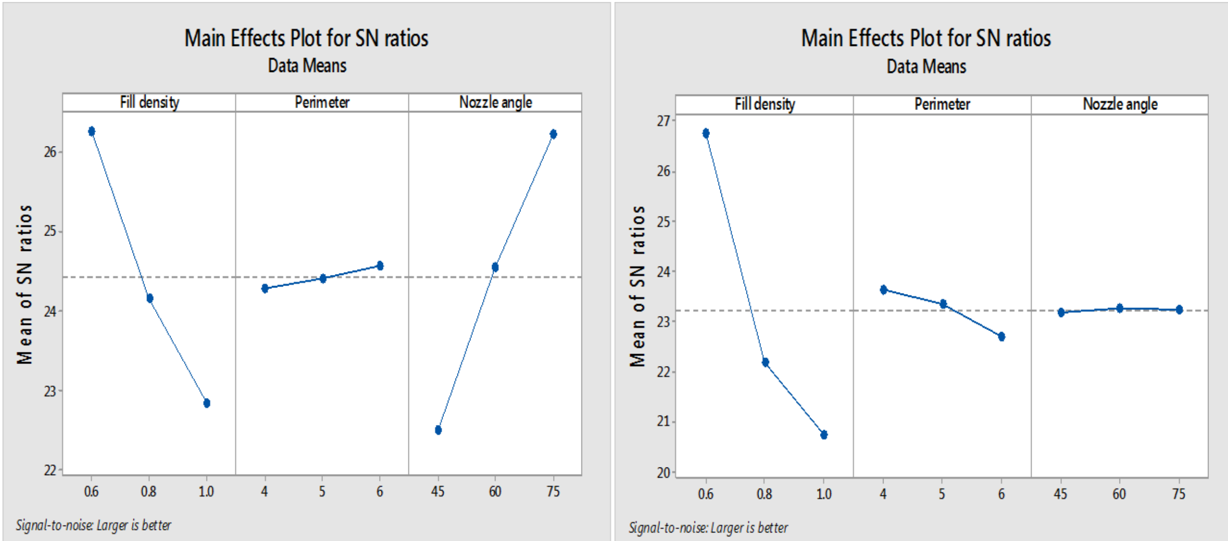

(a) SN ratio lot for ABS-15Al (b)SN ratio plot for PA6-50Al

Fig. 10 Combined SN ratio plot for ABS-15Al and PA6-50Al

3.3 Morphological analysis

SEM analysis has been performed taking fracture surfaces of ABS-15Al and PA6-50Al. For ABS -15Al, overall SN ratio was achieved maximum for experiment no. 3 and minimum at experiment no. 6 (See Table 12). Therefore sample at experiment no. 3 considered best sample and sample at experiment no. 6 has been considered as worst sample. Similarly considering results of Table 12 for PA6-50Al, experiment no. 6 has been selected as best set of experiment and experiment 3 was worst set of experimental setup.

The SEM images were observed at magnification of 200X to justify the compatibility of the parts prepared by FDM in terms of morphological observation. It was observed that ABS-15Al part with best mechanical properties resulted in the brittle fracture characteristics, the dispersion of Al particles was uniform through the surfaces may this is one the reason that this set of part attained maximum tensile strength. Although ABS-15Al part with low tensile resulted in un-uniform dispersion of Al resulted in the less tensile strength attainment. For parts of PA6-50Al, it was observed that overall brittle fracture was received but at the end of the pores of the surfaces tiny ductile fracture resulted. The hole/pores and micro cracks were observed lesser for PA6-50Al (Best) surfaces as compared to PA6-50Al (Worst) part (See Fig. 11).

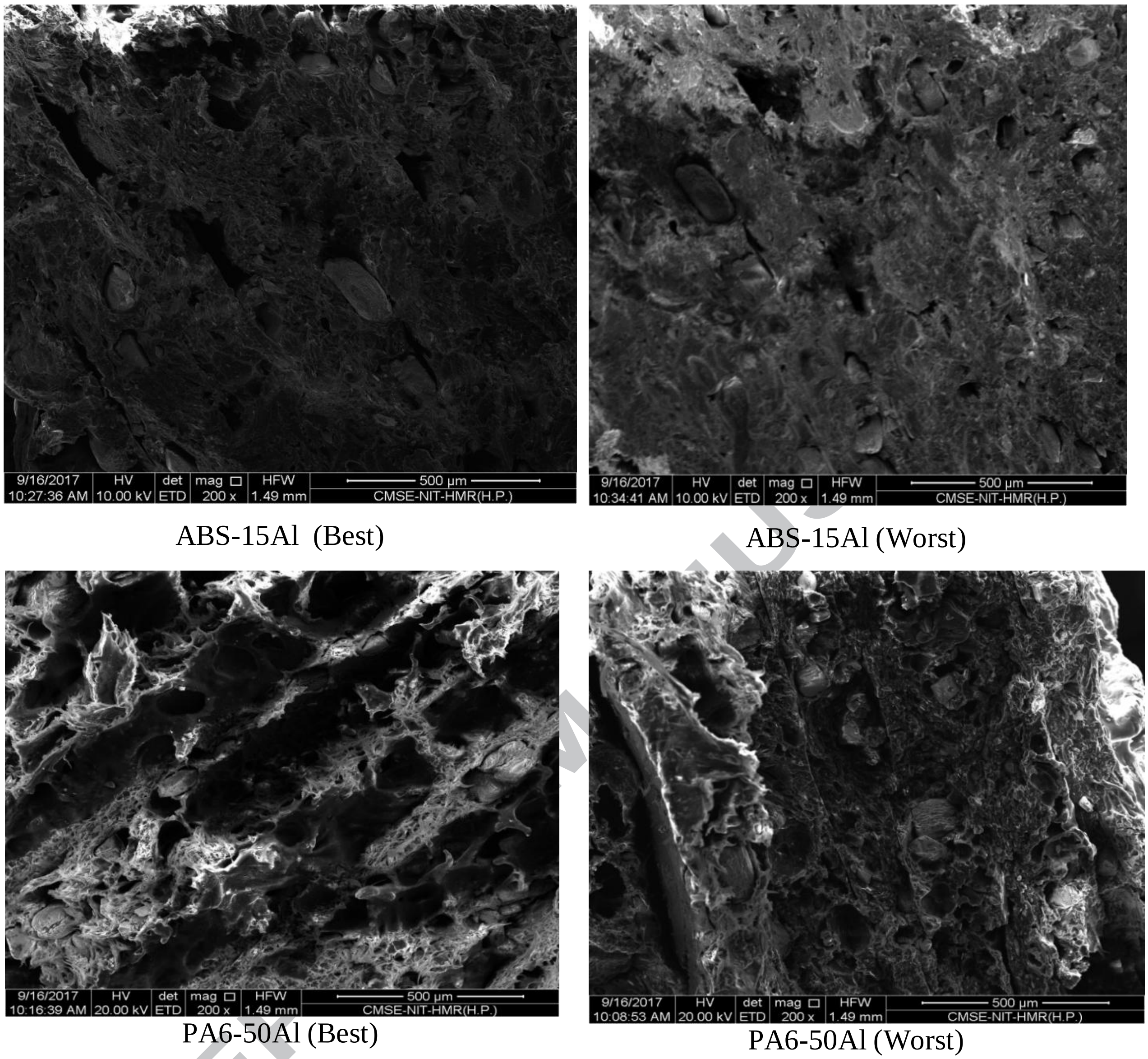

Fig. 11 SEM images for fractured specimen of ABS-15Al and PA6-50Al

3.4 Friction welding operation

Selecting the best set of FDM process parameter firstly there are 2 different cylindrical specimen of ABS-15Al and PA6-50Al have been prepared of dimension 50mmlength and 30mm diameter. After that friction welding was performed under rotational speed of 1200rpm, feed rate of 0.045mm/min, stirring time of 10 seconds on the center lathe. The welding performed under this parametric condition was successful and welded joints were appeared strong physically and visually. So finally it was taken to the consideration that welding of two dissimilar plastic can be achieved by characterizing their melt flow properties. Fig. 12 shows welded piece of ABS-15Al and PA6-50Al.

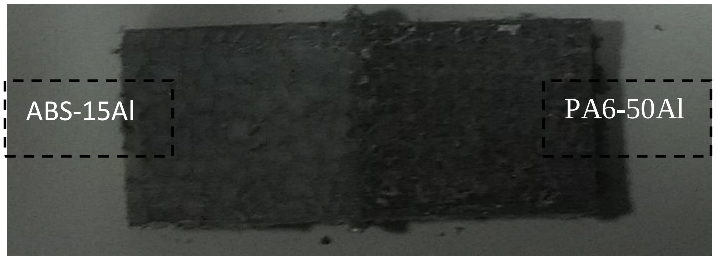

Fig. 12 Welded piece of FDM fabricated

4. Conclusions

The present study was conducted to enhance the compatibility of the two dissimilar thermoplastic materials for friction welding applications by maintain their melt flow properties. Following conclusions can be drawn from present study:

- Welding of ABS and PA6 parts was unsuccessful due to the dissimilarities in their melt flow properties. The reinforcement of 15% Al powder to ABS and 50% Al powder to PA6 matrix resulted in the similar range of MFI (i.e. 11.57g/10min for ABS-15%Al and 11.97g/10min for PA6-50%Al) and finally it has been observed that welding of metal powder reinforced polymers is feasible.
- The reinforcement of 15% Al powder in ABS led to increase in the melting point from 201.22^{o}C to 218.11^{o}C and reinforcement of 50% Al powder to PA6 led to modification in the melting point from 218.35^{o}C to 218.27^{o}C. The reinforcement resulted into the material thermally compatible for friction welding applications.
- As regards to the combined optimization for ABS-15%Al parts is concerned, tensile strength was observed better by keeping fill density of 1.0, no. of perimeter to 6 and nozzle angle of 75^{o}. For PA6-50%Al, the maximum tensile properties were obtained by keeping fill density 1.0, no. of perimeter 4 and nozzle angle of 60^{o}.
- Finally based upon observations of extrusion, FDM and welding operations, it can be concluded that different polymers can be subjected to friction welding only after they have compatible rheological properties.

Acknowledgement: The authors are thankful to BRNS (DAE, GOI), UGC (GOI) for financial support and Punjabi University,Patiala (Mech. Engg. Dept.), Manufacturing Research Lab, GNDEC Ludhiana (Prod. Engg. Dept.) for technical support.

References

[1] Singh, R.; Kumar, R.; Feo, L., and Fraternali, F. Friction welding of dissimilar plastic/polymer materials with metal powder reinforcement for engineering applications. *Composites Part B: Engineering* ***2016***, 101, 77-86.

[2] Kumar, R.; Singh R. and Ahuja IPS. A framework for welding of dissimilar polymers by using metallic fillers. *International Journal of Materials Science and Engineering (IJMSE)***2017**, 8(1), 101-105.

[3] Singh, R.; Kumar, R.; Hashmi MSJ. Friction Welding of Dissimilar Plastic-Based Material by Metal Powder Reinforcement. *Reference Module in Materials Science and Materials Engineering* ***2016***, 13, 1–16.

[4] Singh, R.; Kumar, R.; Hashmi MSJ. Development of graphene blended low cost feedstock filament for FDM. *Reference Module in Materials Science and Materials Engineering* ***2017***, In press

[5] Singh, R.; Kumar, R.; Kumar, S. Polymer Waste as Fused Deposition Modeling Feed Stock Filament for Industrial Applications. *Reference Module in Materials Science and Materials Engineering, Oxford: Elsevier;* ***2017***, 1-12.

[6] Puyvelde, P.V.; Velankar, S. and Moldenasers, P. Rheology and morphology of compatibilized polymer blends. *Current Opinion in Colloid & Interface Science* **2001**, 1(1), 457-463.

[7] Chaitanya, S.; & Singh, I. Processing of PLA/sisal fiber biocomposites using direct-and extrusion-injection molding. *Materials and Manufacturing Processes* **2017**, *32*(5), 468-474.

[8] Wan; Y.; Tang, B.; Liu, C.; Gao, Y., & Jiang, S. Effect of Dy and Nd on ZK10 alloy processed by hot extrusion. *Materials and Manufacturing Processes* **2017**, 1-3.

[9] Hamad, K.; Kaseem M.; Deri F. and Ko, Y.G. Mechanical properties and compatibility of polylactic acid/polystyrene polymer blend. *Materials Letters* **2015**, http://dx.doi.org/10.1016/j.matlet.2015.11.029

[10] Maroufkhani, M.; Katbab, A., Liu, W. and Zhang, J. Polylactide (PLA) and acrylonitrile butadiene rubber (NBR) blends: The effect of ACN content on morphology, compatibility and mechanical properties. *Polymer* **2017**, 115, 37-44.

[11] Nguyen, Q.T.; Ngo, T.; Tran, P.; Mendis, P.; Zobec, M. and Aye, L. Fire performance of prefabricated modular units using organo clay/glass fibre reinforced polymer composite. *Construction and Building Materials* **2016**, http://dx.doi.org/10.1016/j.conbuildmat.2016.10.100

[12] Reyes-labarta, J.A.; Olaya, M.M. and Marcilla A. DSC and TGA study of the transitions involved in the thermal treatment of binary mixtures of PE and EVA copolymer with a crosslinking agent. *Polymer* **2006**, 47, 8194-8202.

[13] Stark, W. and Jaunich, M. Investigation of Ethylene/Vinyl Acetate Copolymer (EVA) by thermal analysis DSC and DMA. *Polymer Testing* 2011, 30, 236-242.

[14] Gao J.; Li C.; Shilpakar U.; Shen Y. Improvements of mechanical properties in dissimilar joints of HDPE and ABS via carbon nanotubes during friction stir welding process. *Material Design* **2015**, 86, 289-296.

[15] Das, C. K.; Nayak, G. C.; Friedrich, S.; & Gehde, M. Vibration welding of amorphous thermoplastic nanocomposites. *Materials and Manufacturing Processes* **2012**, *27*(7), 786-790.

[16] Pal, K.; Panwar, V., Friedrich, S.; & Gehde, M. An Investigation on vibration welding of amorphous and semicrystalline polymers. *Materials and Manufacturing Processes* **2016** , *31*(3), 372-378.

[17] Rajesh, S.; & Badheka, V. Influence of heat input/multiple passes and post weld heat treatment on strength/electrochemical characteristics of friction stir weld joint. *Materials and Manufacturing Processes* **2017**, 1-9.

[18] Rathee, S.; Maheshwari, S.; & Siddiquee, A. N. Issues and strategies in composite fabrication via friction stir processing: A review. *Materials and Manufacturing Processes* **2017**, 1-23.

[19] Chinnadurai, T.; Arungalai Vendan, S.; Rusu, C. C., & Scutelnicu, E. Experimental investigations on the polypropylene behavior during ultrasonic welding. *Materials and Manufacturing Processes* **2017**, 1-9.

[20] Banjare, P. N.; Sahlot, P.; & Arora, A. An assisted heating tool design for FSW of thermoplastics. *Journal of Materials Processing Technology* **2016**, https://doi.org/10.1016/j.jmatprotec.2016.07.035

[21] Yeh, R. Y.; & Hsu, R. Q. "Development of ultrasonic direct joining of thermoplastic to laser structured metal", *International Journal of Adhesion and Adhesives* **2016**, *65*, 28–32.

[22] P., A. K.; Yadav, D.; Perugu, C. S.; and Kailas, S. V. Influence of particulate reinforcement on microstructure evolution and tensile properties of in-situ polymer derived MMC by friction stir processing. *Materials & Design* **2017**, *113*, 99–108.

[23] Ferg, E. E., & Bolo, L. L. (2013). A correlation between the variable melt flow index and the molecular mass distribution of virgin and recycled polypropylene used in the manufacturing of battery cases. *Polymer Testing*, *32*(8), 1452-1459.

[24] Bremner, T., Rudin, A., & Cook, D. G. (1990). Melt flow index values and molecular weight distributions of commercial thermoplastics. *Journal of Applied Polymer Science*, *41*(7- 8), 1617-1627.

[25] Dutta, A. (1984). On viscosity—melt flow index relationship. *Rheologica acta*, *23*(5), 565-569.

[26] Nichetti, D., & Manas-Zloczower, I. (1998). Viscosity model for polydisperse polymer melts. *Journal of rheology*, *42*(4), 951-969.

[27] Shenoy, A. V., Chattopadhyay, S., & Nadkarni, V. M. (1983). From melt flow index to rheogram. *Rheologica Acta*, *22*(1), 90-101.

[28] Teresa Rodríguez- Hernández, M., Angulo- Sánchez, J. L., & Pérez- Chantaco, A. (2007). Determination of the molecular characteristics of commercial polyethylenes with different architectures and the relation with the melt flow index. *Journal of applied polymer science*, *104*(3), 1572-1578.

[29] Ariff, Z. M., Ariffin, A., Jikan, S. S., & Rahim, N. A. A. (2012). Rheological behaviour of polypropylene through extrusion and capillary rheometry. In *Polypropylene*. InTech.